Magnetic-susceptibility studies of graphite intercalation compounds

N.-C. Yeh,* K. Sugihara,† and M. S. Dresselhaus‡
Center for Materials Science and Engineering, Massachusetts Institute of Technology, Cambridge, Massachusetts 02139

G. Dresselhaus
Francis Bitter National Magnet Laboratory, Massachusetts Institute of Technology, Cambridge, Massachusetts 02139
(Received 3 June 1988)

Studies of the temperature (T) and magnetic field (H) dependence of the magnetic susceptibility (χ) for the nonmagnetic donor graphite intercalation compounds (GIC's, K-GIC's and KH_x-GIC's) are focused on three effects. First, an anomalous temperature dependence observed at low temperature and high magnetic field is attributed to inter-Landau-level transitions near the Fermi energy (E_F). Since the Landau-level separation of these quasi-two-dimensional electronic systems is energy dependent, we relate the Fermi energies to the temperature T_s, where $k_B T_s \simeq \Delta_B(E_F,H)$, and Δ_B is the Landau-level separation, which is dependent on both the energy and the external magnetic field. Second, in the low-magnetic-field limit where the Landau-level separation can be neglected, the stronger enhancement of the paramagnetism for higher-stage-donor GIC's with decreasing temperature is attributed to the c-axis charge inhomogeneity. The screening effect on the interior graphite layers is estimated from the temperature dependence of the susceptibility. Third, we compare the room-temperature magnetic-susceptibility values of K-GIC's and KH_x-GIC's considering both the Fermi energy and the c-axis charge distribution. The enhanced Pauli spin susceptibility of these GIC's, due to Fermi-liquid-theory effects, is shown to be significant.

I. GENERAL BACKGROUND

The theory of the magnetic susceptibility for nonmagnetic metals is a complicated problem which includes the response to an external magnetic field from the free-electron spins, bound-electron spins, orbital motion of Bloch electrons, electron spin-orbit coupling, nuclear spins, and hyperfine interaction.

The orbital motion of band electrons in metals is generally the most complicated type of contribution to the susceptibility, since it involves the band structures of the metals, and has to be considered separately for each individual system. Nevertheless, the orbital magnetic susceptibility provides useful information about the band structure of a metal, and therefore is of special interest.

The simplest case of a one-band orbital magnetic susceptibility is the Landau-Peierls magnetic susceptibility ($\chi_{\rm LP}$),[1,2] which is given by the following expression:

$$\chi_{\rm LP}=\frac{e^2}{48\pi^3\hbar^2c^2}\times\sum_l\int d^3k\left[\frac{\partial^2\varepsilon_l}{\partial k_x^2}\frac{\partial^2\varepsilon_l}{\partial k_y^2}-\left[\frac{\partial^2\varepsilon_l}{\partial k_x\partial k_y}\right]^2\right]\times\frac{\partial}{\partial\varepsilon_l}f(\varepsilon_l)\ , \tag{1}$$

where the ε_l are all the energy eigenvalues, $f(\varepsilon_l)=\{\exp[\beta(\varepsilon_l-\mu)]+1\}^{-1}$ is the Fermi-Dirac distribution function, and μ is the chemical potential or Fermi energy. Both of these orbital susceptibility calculations[1,2] assume noninteracting electrons. In 1970, Fukuyama[3] reconsidered the orbital magnetic susceptibility of Bloch electrons using a Green's-function method. The formula he obtained includes many-body effects as well as both interband and intraband transitions. The $\chi_{\rm orb}$ calculated by Fukuyama is

$$\chi_{\rm orb}=\left[\frac{e}{\hbar c}\right]\frac{k_BT}{4\pi^3}\sum_n\int d^3k\ {\rm Tr}\{\mathcal{G}\gamma_x\mathcal{G}\gamma_y\mathcal{G}\gamma_x\mathcal{G}\gamma_y\}\ , \tag{2}$$

where $\mathcal{G}$ is the thermal Green's function defined as

$$\mathcal{G}=(\varepsilon_n I-\mathcal{H})^{-1}\ , \tag{3}$$

and

$$\varepsilon_n=(2n+1)\pi i k_BT+\mu\ , \tag{4}$$

where I is the unit matrix, $n=\ldots,-2,-1,0,1,2,\ldots$, and $\mathcal{H}$ is the Hamiltonian for the electrons in the tight-binding approximation, i is the unit imaginary, and $\gamma_x=(\partial/\partial k_x)\mathcal{H}$, $\gamma_y=(\partial/\partial k_y)\mathcal{H}$ are the momentum operators multiplied by a reciprocal effective-mass factor of $\hbar/m_e^*$, provided the magnetic field is applied along the z axis.

In the case of pristine graphite, the orbital magnetic susceptibility $(\chi_{\parallel})_{\rm orb}$ for $\mathbf{H}\|\hat{\mathbf{c}}$ axis exhibits an unusually large diamagnetic susceptibility (-21.1 emu/g at room temperature), which cannot be explained solely by the Landau-Peierls contribution to the susceptibility.

The mathematical formalism of the orbital susceptibility of graphite was first obtained by McClure,[4] and his analysis yields the following expression in units of $1/{\rm cm}^3$:

$$\chi_{MC}(T) = -\frac{0.044}{k_B T \rho}\left[\frac{4}{\pi c_0}\right]^{3/2}(\gamma_0 a)^2\left[\frac{e}{\hbar c}\right]^2 \times \mathrm{sech}^2\left[\frac{\mu}{2k_B T}\right], \quad (5)$$

where ρ is the density of graphite in units of g/cm^3, μ is the chemical potential of the electron system measured from the $T=0$ Fermi energy E_F, c_0 and a are, respectively, the c-axis repeat distance and the in-plane lattice constant of graphite ($c_0=6.70$ Å and $a=2.46$ Å), and γ_0 (~ 3.1 eV) is the in-plane nearest-neighbor overlap integral in the tight-binding approximation. The strong diamagnetism of graphite results from the interband contributions from π electrons.[4] These interband contributions are actually the inter-Landau-level matrix elements between Landau levels close to $\mu=0$ (i.e., the Fermi energy at $T=0$).

In contrast to the large diamagnetic orbital susceptibility in pristine graphite due to the interband terms[4] and the weak diamagnetism in acceptor-GIC's (graphite intercalation compounds) as expected for normal metals, an unusual paramagnetism in low-stage alkali-metal GIC's was observed by DiSalvo *et al.*[5] The theoretical explanation for this anomaly was first provided by Safran *et al.*[6] The basic concept is that the paramagnetism is associated with the special band structure of the intercalation compounds near the M-point saddle-point singularity of the graphitic Brillouin zone.[6] Since the Landau-Peierls susceptibility strongly depends on the curvature of the energy bands, and the effective masses along the k_x and k_y axes [$m_{xx}=\hbar^2(\partial^2\varepsilon/\partial k_x^2)^{-1}$; $m_{yy}=\hbar^2(\partial^2\varepsilon/\partial k_y^2)^{-1}$] are opposite in sign because of the saddle-point-type singularity in the energy dispersion relation at the M point, the single-band orbital magnetic susceptibility acquires a positive sign, in contrast to normal parabolic dispersion relations in isotropic metals, which give rise to a negative Landau-Peierls susceptibility. Calculations of the susceptibility based on single-layer graphitic bands were done by Blinowski and Rigaux,[7] taking account of both nearest-neighbor and next-nearest-neighbor interactions. Blinowski and Rigaux pointed out that the inclusion of the next-nearest-neighbor interaction accounts for the enhancement of the orbital paramagnetism in donor-GIC's, in contrast to the reduction of the orbital paramagnetism in acceptor-GIC's.[7] Although Blinowski and Rigaux were able to qualitatively explain the paramagnetic total susceptibility in low-stage donor-GIC's, and the diamagnetic total susceptibility in nonmagnetic acceptor-GIC's, the calculated values were too small to explain the experimental data in K-GIC's.[5]

Saito[8] further extended the susceptibility calculations by including the contributions from the interlayer band parameters. This extension is found to be especially important in accounting for the enhancement of the orbital paramagnetism in higher-stage ($n \geq 2$) donor-GiC's. But the theoretical calculations for χ_{orb} after including the multi-graphite-layer contributions were still consistently smaller than the susceptibility obtained by subtracting the core, χ_{core}, and spin, χ_s, contributions from the total measured susceptibility.[8]

The failure to obtain quantitative agreement between Saito's calculation and the experimental data may be explained by taking into account the exchange enhancement of the Pauli spin susceptibility due to many-body effects. This concept appears to be more appropriate here because the orbital magnetic susceptibility based on the Fukuyama formula is a many-body approach. In addition, the exchange enhancement becomes more important for a dilute electron gas if the Hartree-Fock approximation is employed. (This point will be discussed in more detail in Sec. IV.) Consequently, the ratio $(\chi_{\parallel})_{orb}/\chi_s$ (where χ_s denotes the Pauli spin susceptibility) estimated from experiments on K-GIC's,[5] which increases sharply with increasing stage index, should be effectively smaller and should peak at a lower stage than that which DiSalvo *et al.* calculated in GIC's with lower carrier densities. It should be emphasized that the theories of χ_{orb} for GIC's (Refs. 6–8) are calculated in the zero-magnetic-field limit ($H \to 0$), and the temperature dependence of $\chi_{orb}(T)$ in the limit where the Landau-level separation is comparable to the thermal energy has not yet been explained.

In this paper we present temperature- and magnetic-field-dependent susceptibility data for stage-1,2 potassium-hydrogen intercalated graphite (KH_x-GIC's) and stage-1,2 potassium intercalated graphite (K-GIC's). The physics of the studies of KH_x-GIC's is that the relatively strong electron affinity of hydrogen in KH_x-GiC's greatly reduces the charge transfer to the graphite conduction bands from the potassium donor, resulting in electronic properties intermediate between K-GIC's and pristine graphite.[9–11] This special character of KH_x-GIC's provides an advantage of using the Blinowski-Rigaux approach to the calculation of χ_{orb}, because the lower charge transfer to the graphite π conduction bands reduces the inhomogeneous c-axis charge distribution for higher stages ($n \geq 2$),[8] thereby reducing the contribution from the interplanar graphite-graphite coupling to the orbital susceptibility. The enhancement of paramagnetism at low temperatures in higher-stage GIC's ($n \geq 3$) in the low-field limit is also explained by the inhomogeneous c-axis charge distribution. This inhomogeneity is due to the screening effect from the charge in the graphite bounding layers on the graphite interior layers.

Furthermore, in this paper we modify the Fermi-liquid theory to calculate the enhancement of the Pauli spin susceptibility (χ_s) for GIC's, and then show that the exchange enhancement of χ_s is not negligible.

Finally, we show that in the limit where the Landau-level separation Δ_B at E_F becomes comparable to the thermal energy, the anomalous temperature dependence of M/H in these quasi-two-dimensional electronic systems is related to the inter-Landau-level matrix elements near the Fermi energy. Since the Landau-level separation in a two-dimensional system is a function of energy, these anomalies provide us with a way of probing the Fermi energies of the donor-GIC's.

II. EXPERIMENTAL DETAILS

Stage-1 and stage-2 KH_x-GIC's based on highly oriented pyrolytic graphite (HOPG) were prepared using a

two-zone method under the conditions mentioned elsewhere.[9] A typical size of these samples after intercalation is about $4\times4\times2$ mm^3. The stage index and stage fidelity of these samples were characterized using a $(00l)$ x-ray diffractometer. The $(00l)$ diffractograms, indicating stage-1 KH_x-GIC's with interplanar repeat distance $I_c=8.55\pm0.03$ Å and pure stage-2 KH_x-GIC's with $I_c=11.92\pm0.03$ Å, are presented elsewhere.[9,12]

The dc magnetic susceptibility was measured using a SQUID (superconducting quantum interference device) magnetometer. The sensitivity of the measured magnetic moments from the SQUID magnetometer is better than 10^{-9} emu/g. The air-sensitive KH_x-GIC samples, typically with net weight of tens of mg, were mounted in a Teflon sample holder using an argon-gas-filled glove bag. The sample holder was then sealed with 5-min epoxy before being taken out of the glove bag.[12] All these samples were characterized again using $(00l)$ x-ray diffraction after the SQUID measurements, to ensure that the condition of the samples remained stable during the experiments. The SQUID magnetometer allows measurement of the total magnetic moment of the sample as a function of temperature and magnetic field. The temperature range of these measurements was between 6 and 300 K, and the dc magnetic field range between 0 and 5 T. The accuracy of the temperature reading is better than 0.1 K, and that for the magnetic field reading is better than 10^{-3} T in our measurements. Since the total moments of these nonmagnetic GIC's are very small, typically on the order of 10^{-6} emu/g, a correction to the data from the background (sample holder plus epoxy) is very important. All the measurements done on the samples were repeated on the background, and the net signals from the samples were obtained by subtracting the background data from the total moments. The results for stage-1 KH_x-GIC's were averaged over the measurements on four samples, and those for stage-2 KH_x-GIC's were averaged over the measurements taken on three samples. The variation of $\chi_\parallel(T)$ among samples with the same chemical composition but from different batches is less than 30% of the average value.

Similar measurements were also done on K-GIC's and pristine graphite, and were compared to other measurements reported by other groups using a Faraday balance apparatus.[5] The low-magnetic-field data from these control samples were consistent with other measurements.[5] The measurements of the magnetic susceptibility of these controlled samples (K-GIC's) were carried out on a stage-1 C_8K, a stage-2 $C_{24}K$, and a pristine HOPG sample. Since only the magnetic susceptibility with applied field $\mathbf{H}\|\hat{\mathbf{c}}$ axis provides interesting information on the orbital susceptibility, we focused our studies on the measurements with this orientation. It should be noted that the demagnetization factor due to the anisotropic geometry of the samples does not significantly affect the in-plane magnetic-susceptibility data for this field orientation, because the susceptibility with $\mathbf{H}\|\hat{\mathbf{c}}$ axis ($\chi_\parallel^0$) is much larger than that with $\mathbf{H}\perp\hat{\mathbf{c}}$ axis ($\chi_\perp^0$), and the measured in-plane susceptibility ($\chi_\parallel$) satisfies the following condition:

$$\chi_\parallel=\frac{\chi_\parallel^0+\kappa\chi_\perp^0}{1+\kappa}\ , \tag{6}$$

where $0<\kappa\ll1$ and $\chi_\perp^0\ll\chi_\parallel^0$. Therefore $\chi_\parallel\simeq\chi_\parallel^0$. Typically, $\kappa\leq0.02$ in the case of pristine graphite, and $\kappa<0.1$ for GIC's.[5]

In this paper the dc magnetic susceptibility in the measurements was obtained by dividing the measured moments by the applied field and the sample weight. The values for K-GIC's thus obtained are consistent with other measurements in the low-magnetic-field limit (which we take as $H\leq0.5$ T). On the other hand, as the magnetic field becomes sufficiently high to induce a nonlinear effect, the dc magnetic susceptibility (M/H) exhibits deviations from the values obtained from the definition $\chi\simeq\Delta M/\Delta H$, where ΔH is sufficiently small.

III. EXPERIMENTAL RESULTS

Figures 1–5 show plots of the c-axis magnetic susceptibility ($\chi_\parallel$) versus temperature (T) at various static magnetic fields: Fig. 1 for stage-1 KH_x-GIC's, Fig. 2 for stage-2 KH_x-GIC's, Fig. 3 for stage-1 K-GIC's, Fig. 4 for stage-2 K-GIC's, and Fig. 5 for pristine graphite (HOPG). There are several interesting features in these figures. Firstly, for all the GIC's measured, the magnetic susceptibility in the high-temperature range [the high-temperature range is defined by $k_BT>\Delta_B(E_F,H)$, where $\Delta_B(E_F,H)$ is the Landau-level separation at the Fermi energy E_F] is paramagnetic, in contrast to $\chi_\parallel$ for pristine graphite, which is diamagnetic. The absolute values of the dc magnetic susceptibility ($\chi\equiv M/H$) decrease with increasing magnetic field.

Secondly, the magnetic susceptibility of GIC's is constant in the high-temperature limit (Figs. 1–4), in contrast to that of pristine graphite (Fig. 5). Thirdly, all the traces for the GIC's shown in Figs. 1–4 exhibit an interesting temperature dependence in the low-temperature

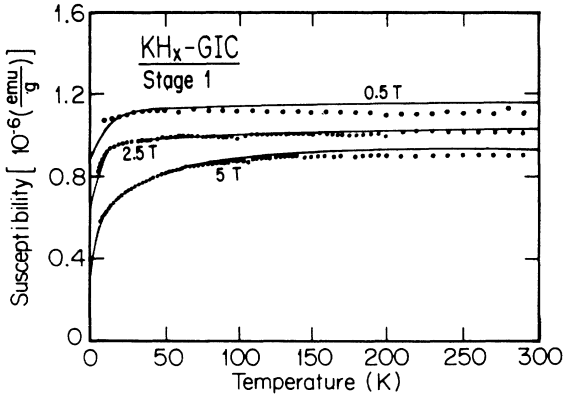

FIG. 1. The temperature dependence of the magnetic susceptibility [$\chi_\parallel(T)$] for stage-1 KH_x-GIC's at magnetic fields of 0.5, 2.5, and 5.0 T. The dots are the experimental data averaged over three samples and the solid lines are the theoretical fits [Eq. (27)] to the experimental data.

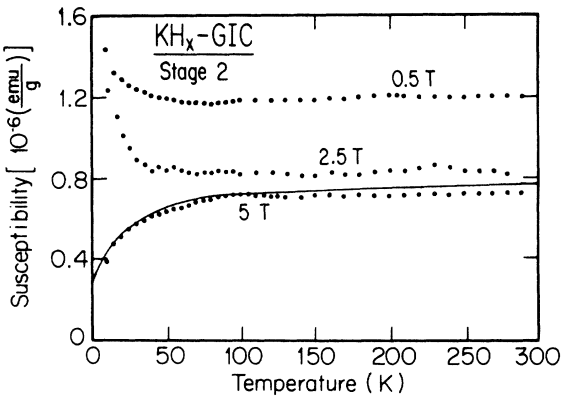

FIG. 2. The temperature dependence of the magnetic susceptibility $[\chi_{\|}(T)]$ for stage-2 KH_x-GIC's at magnetic fields of 0.5, 2.5, and 5.0 T. The dots are the experimental data averaged over two samples and the solid line is the theoretical fit [Eq. (27)] to the experimental data at 5.0 T.

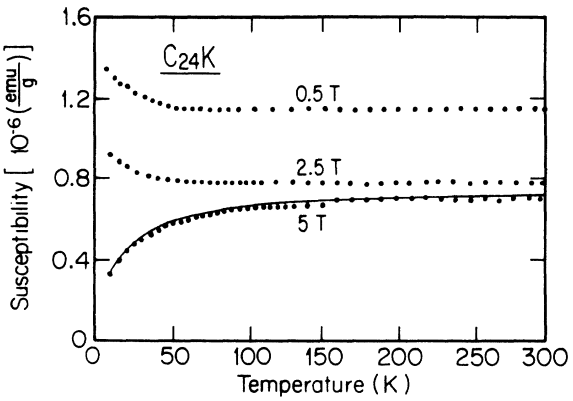

FIG. 4. The temperature dependence of the magnetic susceptibility $[\chi_{\|}(T)]$ for a stage-2 K-GIC at magnetic fields of 0.5, 2.5, and 5.0 T. The dots are the experimental data and the solid line is the theoretical fit [Eq. (27)] to the experimental data at 5.0 T.

region. The magnetic susceptibility shows an anomalous decrease in paramagnetism for both the stage-1 KH_x-GIC's and K-GIC's in the low-temperature region for the entire range of applied magnetic fields, and the magnitude of the anomaly increases with increasing magnetic field (Figs. 1 and 3). In contrast, the magnetic susceptibility for both the stage-2 KH_x-GIC's and K-GIC's exhibits an *increase* in paramagnetism in the low-temperature region for smaller magnetic fields (Fig. 2 and 4), while an anomalous *decrease* in paramagnetism is also observed as the external magnetic field becomes sufficiently large (Fig. 2 at 5 T and Fig. 4 at 5 T). The anomalous decrease in paramagnetism for donor-GIC's in the high-field and low-temperature limit is a specially interesting phenomenon, and will be explored in detail later.

The $\chi_{\|}(T)$ data in the low-field limit ($H \leq 0.5$ T) for both KH_x-GIC's and K-GIC's are plotted in Fig. 6 for comparison, and the room-temperature values are listed in Table I. The $\chi_{\|}(T)$ traces for the stage-3 and stage-4 K-GIC's in Fig. 6 were taken by DiSalvo *et al.*,[5] and not by the present authors. Also note that both the stage-3 and stage-4 K-GIC's exhibit an increase in paramagnetism in the low-temperature region. Good agreement is obtained between our measurements on the stage-1 and stage-2 K-GIC's and those reported by DiSalvo *et al.*[5]

To discuss these data we define two characteristic temperatures T_s and T_0. For all the $\chi_{\|}(T)$ traces showing a decrease in paramagnetism at low T, we define the saturation temperature T_s as

$$[\chi_{\|}(T_s)-\chi_{\|}(0)] \equiv 0.5[\chi_{\|}(300\ \text{K})-\chi_{\|}(0)] , \tag{7}$$

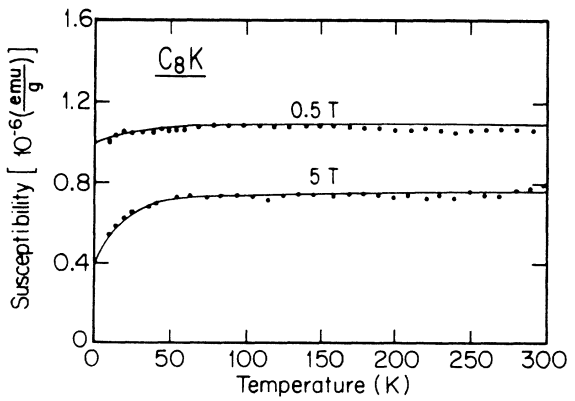

FIG. 3. The temperature dependence of the magnetic susceptibility $[\chi_{\|}(T)]$ for a stage-1 K-GIC at magnetic fields of 0.5 and 5.0 T. The dots are the experimental data and the solid lines are the theoretical fits [Eq. (27)] to the experimental data.

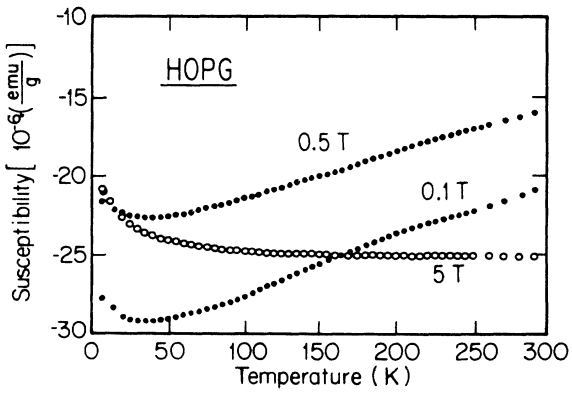

FIG. 5. The temperature dependence of the magnetic susceptibility $[\chi_{\|}(T)]$ for pristine HOPG at magnetic fields of 0.1, 0.5, and 5.0 T.

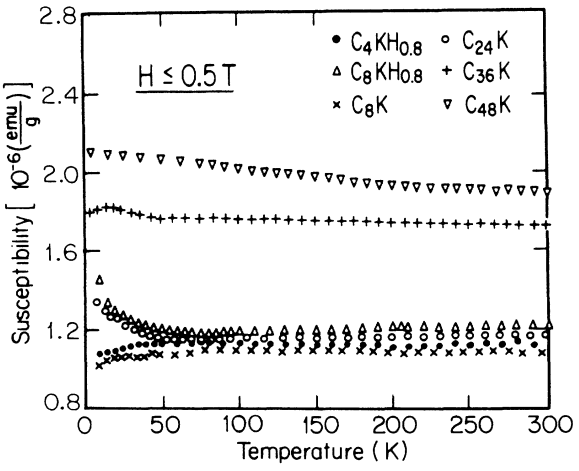

FIG. 6. Comparison of the magnetic susceptibility $[\chi_{\parallel}(T)]$ between KH_x-GIC's and K-GIC's for $H \leq 0.5$ T of stage-1 KH_x-GIC's (●), stage-2 KH_x-GIC's (△), stage-1 K-GIC's (×), stage-2 K-GIC's (○), stage-3 K-GIC's (Ref. 5) (+), and stage-4 K-GIC's (Ref. 5) (▽). The measurements for the stage-3 and stage-4 samples are from Ref. 5.

where $\chi_{\parallel}(0)$ represents an extrapolation to the low-temperature limit from the experimental data. For the traces of $\chi_{\parallel}(T)$ showing an increase in paramagnetism at low T, we define T_0 as

$$|\chi_{\parallel}(300\text{K}) - \chi_{\parallel}(T_0)| \equiv 0.1\chi_{\parallel}(300\text{ K}) . \quad (8)$$

The values for T_s and T_0 for both K-GIC's and KH_x-GIC's at various fields are listed in Table II, and the physical meaning of the characteristic temperatures T_s and T_0 is discussed below.

An intuitive explanation for the decrease in the magnitude of $\chi_{\parallel}$ at high field and low temperature ($T < T_s$) is as follows. The thermally induced transitions from the occupied Landau levels right below the Fermi energy to the unoccupied Landau levels above the Fermi energy give rise to an additional enhancement of the paramagnetism of the Bloch electrons, because the transitions of electrons from the Landau levels below the Fermi energy to those above the Fermi energy result in larger Bloch-electron orbitals which are closer to the saddle point (the M point). These transitions are easier to achieve if the thermal energy of the conduction electrons near E_F is larger than the energy difference Δ_B between consecutive Landau levels near E_F. If the conduction electrons do not possess enough thermal energy, most electrons will remain below the Fermi level, resulting in a larger diamagnetic contribution to the susceptibility. On the other hand, if the Landau-level separation becomes much smaller than the thermal energy, the electron distribution becomes insensitive to the discrete Landau levels, so that the transitions from the energy states below the Fermi level to those above can take place within an energy interval $k_B T$. This explains the gradual decrease of paramagnetism in both stage-1 and stage-2 KH_x-GiC's at low temperature and in the high-magnetic-field limit.

The viewpoint of attributing the temperature dependence of the orbital susceptibility to the inter-Landau-level transitions is furthermore supported by the field-dependent susceptibility data taken on HOPG, as shown in Fig. 5. In the low-temperature region, we note that with the increase of thermal energy the diamagnetism of graphite increases due to the thermal excitations of elec-

TABLE I. Comparison between experimental orbital susceptibility $(\chi_{\text{orb}})^{\text{expt}}$ after the correction to χ_s and the theoretical orbital susceptibility $(\chi_{\text{orb}})^{\text{theor}}$. [All the susceptibility data are in units of 10^{-6} emu/(g of sample). The experimental results for $C_{36}K$ and $C_{48}K$ are from Ref. 5.] Note that $(\chi_{\text{orb}})^{\text{expt}}$ for the stage-1 compounds agrees reasonably well with $(\chi_{\text{orb}})^{\text{theor}}$ after the exchange-enhancement correction is made.

	$\chi_{\parallel}$ [a]	χ_{core} [b]	χ_s [c]	χ_0 [d]	$(\chi_{\text{orb}})^0$ [e]	$(\chi_{\text{orb}})^{\text{theor}}$ [f]	$(\chi_{\text{orb}})^{\text{expt}}$ [g]
$C_4KH_{0.8}$	1.10	−0.37	0.35	0.81	1.12	0.60	0.66
$C_8KH_{0.8}$	1.25	−0.38	0.30	0.51	1.33	0.60	1.07
C_8K	1.02	−0.38	0.48	0.90	0.92	0.50	0.50
$C_{24}K$	1.50	−0.39	0.25	0.41	1.64	0.70	1.48
$C_{36}K$	1.75	−0.39	0.21	0.69	1.93	0.90	1.45
$C_{48}K$	1.87	−0.40	0.20	0.58	2.07	1.10	1.69
HOPG	−21.1	−0.40	0.016	0.016	−21.5	−24.0	−21.5

[a]The values of the total susceptibility here are taken at $T = 300$ K.
[b]The core susceptibility values are -4.8×10^{-6} emu/mol for C, -13×10^{-6} emu/mol for K^+, and -0.018×10^{-6} emu/mol for H^- (Ref. 5), respectively.
[c]The Pauli spin susceptibility is obtained from the electronic specific heat.
[d]Enhanced Pauli susceptibility after Fermi-liquid corrections. The errors in the estimated values lie in the uncertainties of the available f_C, m_e^*, and γ_e.
[e]$(\chi_{\text{orb}})^0$ is defined as $(\chi_{\text{orb}})^0 \equiv \chi_{\parallel} - \chi_{\text{core}} - \chi_s$.
[f]The theoretical orbital susceptibility for K-GIC's is calculated using Saito's formulas (Ref. 8), and that for KH_x-GIC's is obtained using the calculations of Blinowski and Rigaux based on the single-graphite-layer tight-binding approximation (Ref. 7).
[g]The experimental orbital susceptibility is obtained from the formula $(\chi_{\text{orb}})^{\text{expt}} = \chi_{\parallel} - \chi_{\text{core}} - \chi_0$.

TABLE II. Two characteristic temperatures T_s and T_0 for $\chi_{\parallel}(T)$ at various magnetic fields.

	$H=0.5$ T	$H=2.5$ T	$H=5.0$ T	E_F (eV)
$C_4KH_{0.8}$	$T_s \ll 10$ K	$T_s \sim 20$ K	$T_s \sim 25$ K	1.2[a] (1.4)[b]
$C_8KH_{0.8}$	$T_0 \sim 30$ K	$T_0 \sim 30$ K	$T_s \sim 30$ K	1.0[a] (1.1)[b]
C_8K	$T_s \ll 10$ K	$T_s < 10$ K	$T_s \sim 15$ K	2.4[a] (2.6)[c]
C_{24} K	$T_0 \sim 40$ K	$T_0 \sim 30$ K	$T_s \sim 20$K	1.5[a] (1.8)[c]

[a]The Fermi energy E_F is estimated using the formula $E_F \simeq B/k_B T_s$ [see Eq. (28)] and magnetic field $H=5.0$ T.
[b]Reference 13.
[c]Reference 14.

trons from the valence band to the conduction band. As the temperature increases further, more electrons are excited to the conduction band, and larger Bloch-electron orbitals become available. Since the band curvature of the three-dimensional (3D) graphite near the K point begins to deviate from a linear k dependence for larger Bloch-electron orbitals, and the effective masses along the k_x and the k_y axes become opposite in sign, a gradual increase in the paramagnetism takes place at high temperatures. However, if the applied magnetic field becomes sufficiently high to introduce a large Landau-level separation, as in the case of Fig. 5 at 5 T, the thermal energy of electrons in the experimental temperature region becomes too small, so that the transitions are restricted to the interband transitions. Consequently, the magnetic susceptibility at high magnetic fields saturates at high temperatures (Fig. 5 at 5 T), in contrast to a gradual increase in paramagnetism for smaller magnetic fields (Fig. 5).

The physical meaning of the other characteristic temperature T_0 (see Fig. 6 for stage-3 and -4 K-GIC's) can be described as follows. Since the interior graphite layers possess few conduction electrons relative to the bounding layers due to the Coulomb screening effect, the effective chemical potential for the interior layers (μ_{in}) is much smaller than that of the bounding layers. The lower chemical potential of the interior layers results in a small increase of paramagnetism at low temperature, reminiscent of the temperature-dependent susceptibility of pristine graphite at $T < \mu_{\text{in}}/k_B$ (Ref. 4) (see Fig. 5). Since the characteristic temperature T_0 is related to the chemical potential of the interior graphite layers, we may estimate the chemical potential and the screening length of the interior layers from the characteristic temperature T_0, as is discussed further below.

IV. CORRECTIONS TO $\chi_{\parallel}$ OF K-GIC'S USING FERMI-LIQUID THEORY

The exchange enhancement of the Pauli spin susceptibility based on Fermi-liquid theory for $T=0$ yields[15–17]

$$\chi_0 = \frac{m_e^*/m_0}{1+B_0}\chi_s \ , \tag{9}$$

where χ_0 is the enhanced spin susceptibility and B_0 is a negative constant.[15–17] The effective mass of the quasiparticle, m_e^*, for a 3D system with the energy dispersion relation $E(\mathbf{k})=\hbar^2 k^2/2m_0$ is enhanced relative to the band effective mass m_0 by the many-body interaction,[15,17]

$$m_e^* = m_0\left[1+\frac{A_1}{3}\right] , \tag{10}$$

where A_1 is a positive constant which can be determined from the electronic specific heat.[17] However, this effect is not important for GIC's,[12] which exhibit a linear energy dispersion relation, $E(\kappa)\simeq p_0|\kappa a|$, where $\kappa=\kappa_a+\kappa_z\hat{\mathbf{z}}$ and $p_0=\sqrt{3}\gamma_0 a/2$.

Therefore, in the case of GIC's, where $A_1 \ll 1$,[12] the Fermi-liquid-theory effects result in

$$\chi_0 = \frac{1}{1+B_0}\chi_s \ . \tag{11}$$

In the Hartree-Fock approximation,[17] B_0 is related to the band-electron effective mass (m_0) and the Fermi wave vector (k_F) through the expression

$$B_0 = -\frac{m_0 e^2}{\pi\hbar^2 k_F} \ . \tag{12}$$

The negative sign of B_0 is characteristic of the Hartree-Fock approximation which favors parallel spin states. In a dilute system, the antiparallel spin correlation which is neglected in the Hartree-Fock approximation does not contribute significantly to the susceptibility, and therefore the expression for B_0 in Eq. (12) remains valid. As the quasiparticle concentration becomes denser, the increasing Coulomb repulsion force requires consideration of the antiparallel spin correlation. In this case, the Fermi-liquid theory given above has to be modified, and use of the Hubbard model[18] with correction for antiparallel spin correlation in the strong-coupling limit becomes necessary. This type of correction generally leads to a decrease in the Pauli spin enhancement.[17] However, the theories involved in the correction of the spin-exchange enhancement are beyond the scope of this paper. We shall only focus on the Fermi-liquid approach when discussing the susceptibility of GIC's.

If we employ the two-dimensional dispersion relation [$E(\kappa)=p_0|\kappa a|$] for GIC's, the carrier density n_c can be related to k_F and the c-axis repeat distance (I_c) by the following formula:

$$n_c = \frac{g_s g_c}{(2\pi)^3}(\pi k_F^2)\left[\frac{2\pi}{I_c}\right], \tag{13}$$

where g_s is the spin degeneracy and g_c is the number of carrier pockets per reciprocal unit cell. We may therefore rewrite B_0 in terms of the physical quantities associated with donor-GIC's by the formula

$$B_0 = -\frac{m_0 e^2}{\pi^{3/2}\hbar^2 (n_c I_c)^{1/2}} . \tag{14}$$

We define below the charge transfer of graphite to be f_C=charge per C atom for stage-n GIC's, where a positive sign indicates holes and a negative sign indicates electrons. Then f_C can be expressed as

$$f_C = -\frac{g_s g_c \pi k_F^2 (2\pi/I_c)}{2nV_{BZ}} \tag{15}$$

for donor-GIC's, where $V_{BZ}=[(2\pi)^3 2/(\sqrt{3} I_c a^2)]$ is the graphite reciprocal-space unit cell.

In the case of K-GIC's, if the stoichiometry of the carbon-to-potassium ratio is [C]:[K]=x:1, the charge transfer per carbon atom can be related to the charge transfer from potassium (f_K) in the form $|f_C|=f_K/x$. Combining Eqs. (14) and (15), we obtain

$$\begin{aligned} B_0 &= -\frac{3^{1/4}}{2\pi^{3/2}(n|f_C|)^{1/2}}\left[\frac{m_0}{m_e^*}\right]\left[\frac{a}{a_B}\right] \\ &= -\frac{0.55}{(n|f_C|)^{1/2}}\left[\frac{m_0}{m_e^*}\right] \\ &= -0.55\left[\frac{x}{nf_K}\right]^{1/2}\left[\frac{m_0}{m_e^*}\right] . \end{aligned} \tag{16}$$

where $a_B \equiv \hbar^2/(m_e^* e^2)$ is the effective Bohr radius and $a = 2.46$ Å is the graphite in-plane lattice constant.

Since the Pauli spin susceptibility can be obtained from specific-heat measurements, i.e.,

$$\chi_s = \frac{3\mu_B^2 \gamma_e}{\pi^2 k_B^2} , \tag{17}$$

where γ_e is the electronic specific-heat coefficient, we may rearrange the enhanced Pauli susceptibility in terms of available experimental parameters:

$$\chi_0 = \left[\frac{3\mu_B^2\gamma_e}{\pi^2 k_B^2}\right]\left[1-\left[\frac{m_0}{m_e^*}\right]\frac{0.55}{(n|f_C|)^{1/2}}\right]^{-1} . \tag{18}$$

Note that the uncertainty of χ_0 lies in the uncertainty of the available values for f_C, m_0, and γ_e, where f_C and m_0 can be determined from the largest Fermi cross section measured from the Shubnikov–de Haas (SdH) experiments. The comparisons between χ_s and χ_0 for stage-1 KH_x-GIC's and stage-1 K-GIC's are listed in Table I. Although we could also estimate the exchange enhancement of the Pauli susceptibility using Eq. (18), we do not emphasize the significance of these values in Table I, due to uncertainties in the f_C and m_0 values from available experiments. Nevertheless, from the enhanced susceptibility χ_0 in the stage-1 compounds, we conclude that the exchange enhancement to the Pauli spin susceptibility is not negligible in GIC's.

Using this formula, we are able to obtain better agreement between the experimental orbital susceptibility $(\chi_{orb})^{expt}$ and the theoretical orbital susceptibility $(\chi_{orb})^{theor}$ (Table I). Note that $(\chi_{orb})^{expt}$ is defined as

$$(\chi_{orb})^{expt} \equiv \chi_{\parallel} - \chi_{core} - \chi_0 , \tag{19}$$

and $(\chi_{orb})^0$ is the orbital susceptibility without Fermi-liquid corrections:

$$(\chi_{orb})^0 \equiv \chi_{\parallel} - \chi_{core} - \chi_s . \tag{20}$$

The calculated orbital susceptibility $(\chi_{orb})^{theor}$ in Table I for K-GIC's is based on Saito's calculations, which include consideration of the c-axis charge distribution.[8] Also note that the enhancement of χ_s becomes more important for a dilute system (i.e., smaller f_C) under the Hartree-Fock approximation. This may account for the larger discrepancy between $(\chi_{orb})^0$ and $(\chi_{orb})^{theor}$ for higher stages.

All the relevant parameters are listed in Tables I and III. The largest Fermi cross section (ν_{max}) for each donor-GIC, which is assumed to be from the dominant carriers, and the corresponding effective mass (m_0), are determined from the Shubnikov-de Haas experiments. The carrier densities and the charge-transfer ratios (f_C and f_K) are also obtained from SdH measurements. Since the highest SdH frequencies (ν_{max}) in each sample are usually difficult to be detected due to the experimental conditions, and the effective masses are heavier for the carriers associated with higher frequencies, the real enhanced spin susceptibility (χ_0) may be larger in magnitude than what we have estimated here. Apparently the Fermi-liquid corrections are not negligible in view of the above rough estimate.

It is shown in Table I that the agreement between $(\chi_{orb})^{expt}$ and $(\chi_{orb})^{theor}$ is the best for both stage-1 K-GIC's and KH_x-GiC's, while $(\chi_{orb})^{theor}$ is consistently smaller than $(\chi_{orb})^{expt}$ for higher stages, although the discrepancy has already been reduced substantially with the Fermi-liquid correction. Besides the uncertainty in the determination of χ_0, a possible resolution of this problem could lie in the calculations of $(\chi_{orb})^{theor}$, which may be more complicated than the Fukuyama approximation in the case of higher-stage GIC's, because the number of energy bands participating in the orbital magnetism increases with the stage index.

TABLE III. Some important parameters for KH_x-GIC's, K-GIC's, and pristine graphite.

	W^a	$\nu_{max}{}^b$	$f_C{}^c$	$f_K{}^d$	$E_F{}^e$	$(m_e^*)_{max}/m_e^*$
HOPG	12.01				0.02	0.036
$C_4KH_{0.8}$	15.16	680[f]	0.020	0.88	0.89[f] (1.1[g])	0.23[f]
$C_8KH_{0.8}$	13.88	1525[f]	0.025[f]	1.0	1.15[f]	0.17[f]
C_8K	15.02	2870[h]	0.075	0.6	2.65[i]	0.3
$C_{24}K$	13.09	440[j]	0.042	1.0	1.8[i]	0.2
$C_{36}K$	12.74	260[k]	0.01	0.3	1.2	0.15
$C_{48}K$	12.56	338[k]	0.01	0.19	1.1	0.12

[a]Mole weight of samples, in units of g/mol.
[b]Maximal Fermi cross section from Shubnikov–de Haas experiments, in units of T.
[c]In units of number of electrons per carbon atom.
[d]In units of number of electrons per potassium atom.
[e]In units of eV.
[f]Reference 9.
[g]Reference 13.
[h]From the SdH experiments (Ref. 19).
[i]From the optical measurements (Ref. 14).
[j]Reference 20.
[k]Reference 21.

V. THEORETICAL MODELS FOR $\chi_{\parallel}(T,H)$ OF KH_x-GIC'S

In the preceding section we focused on the room-temperature values of $(\chi_{\parallel})_{tot}$ for various systems in the low-field limit, where the temperature dependence of $\chi_{\parallel}$ was neglected. In this section we shall first examine the origin of the temperature dependence of the magnetic susceptibility. Then we use the formalism derived by Blinowski and Rigaux[7] to obtain the temperature dependence of $\chi_{\parallel}$ for donor-GIC's, and compare the calculated results to the experimental data.

The general calculations of the magnetic susceptibility are usually derived in the low-magnetic-field limit, where one may assume a continuous energy spectrum and the calculation requires an integration over the Brillouin zone. The temperature dependence of the magnetic susceptibility enters from the Fermi-Dirac distribution function for the conduction electrons. This temperature dependence is usually negligible if the applied magnetic field is very small, i.e., if the Zeeman energy is much smaller than the thermal energy $k_B T$.

However, if the Landau-level separation (Δ_B) at the Fermi energy becomes comparable to the thermal energy ($\Delta_B \sim k_B T$), but not large enough to perturb the density of states, an additional correction to the Landau-Peierls susceptibility and Pauli spin susceptibility should be made. This correction comes from the Fermi-Dirac distribution function in the integration of the magnetic susceptibility over the first Brillouin zone, which yields the following temperature dependence:

$$\delta\chi \equiv \delta\chi_{LP} + \delta\chi_s = -\frac{\Delta_B}{4k_B T}(\chi_{LP} + \chi_s) \ . \tag{21}$$

In 3D metals, since $\chi_{LP} < 0$ and $\chi_s > 0$, and $|\chi_{LP}| \sim |\chi_s|$, this correction becomes very small. Generally, it is necessary to know the band structure to obtain the correct estimate for $\delta\chi$. In the case of GIC's, since both χ_{LP} and χ_s are positive, the temperature dependence of the magnetic susceptibility becomes more significant in the limit of $\Delta_B \sim k_B T$. In the case of GIC's, the Landau-level energies for a single-graphene-layer Hamiltonian yield the following relation,[22,23]

$$E_n = \pm\sqrt{(2n+1)B} \ , \tag{22}$$

where $B = \frac{3}{4}(a\gamma_0)^2 s$, and $s = eH/\hbar c$. Here, γ_0 is the nearest-neighbor overlap integral, which is about 3.1 eV for pristine graphite, and $a = 2.46$ Å is the in-plane lattice constant.

The energy difference $\Delta_B(E_n)$ between two consecutive Landau levels is

$$\begin{aligned}\Delta_B(E_n) &= E_{n+1} - E_n \\ &= \sqrt{2B}\,[(n+1)^{1/2} - n^{1/2}] \\ &\simeq \frac{B}{E_n} \ .\end{aligned} \tag{23}$$

The last equation, $\Delta_B(E_n) \simeq B/E_n$, is satisfied provided $n \gg 1$. In fact, this approximation is better than 5% for $n > 3$. If the applied field is in units of T and E in eV, then $\Delta_B(E_n) = (6.2 \times 10^{-4})(H/E_n)$ eV.

An explicit expression for χ_{orb} using Fukuyama's approximation was derived by Blinowski and Rigaux[7] for the single-graphene-layer Hamiltonian. Using the Fukuyama formula in Eq. (2), and inserting the explicit expressions of the momentum operators and the Green's-function matrix elements in that equation, Blinowski and Rigaux obtained the orbital magnetic susceptibility by performing the integration in Eq. (2) over the two-dimensional graphite Brillouin zone:

$$\chi_{\rm orb}=\left[\frac{e}{\hbar c}\right]^2\frac{N_A\Omega\gamma_0 b^2}{32\pi^2}\left[\int_0^3\frac{d\epsilon}{\epsilon^3}[f(E_2-E_F)-f(E_1-E_F)][h_1(\epsilon)-\gamma^2\epsilon^2h_3(\epsilon)+\gamma^2h_4(\epsilon)]\right.$$
$$+\int_0^3\frac{d\epsilon}{\epsilon^2}[h_1(\epsilon)\gamma\epsilon h_2(\epsilon)+\gamma^2\epsilon^2h_3(\epsilon)+\gamma^2h_4(\epsilon)+\gamma^3\epsilon h_5(\epsilon)]\frac{\partial f(E_1-E_F)}{\partial E_1}$$
$$\left.+\int_0^3\frac{d\epsilon}{\epsilon^2}[h_1(\epsilon)-\gamma\epsilon h_2(\epsilon)+\gamma^2\epsilon^2h_3(\epsilon)+\gamma^2h_4(\epsilon)-\gamma^3\epsilon h_5(\epsilon)]\frac{\partial f(E_2-E_F)}{\partial E_2}\right], \quad (24)$$

where $b=a/\sqrt{3}$ and $\epsilon=E/\gamma_0$, $E_1(\epsilon)=\epsilon-\gamma\epsilon^2$, and $E_2(\epsilon)=-\epsilon-\gamma\epsilon^2$, $\gamma\gamma_0$ is the next-nearest-neighbor coupling energy, where γ is a dimensionless constant, and the functions $h_i(\epsilon)$ are defined in Ref. 7, and the limits of integration correspond to the width of the π band.

With the analytical expression [in Eq. (24)] we can proceed to consider the temperature and magnetic field effects on the orbital susceptibility. The basic concept is that the introduction of the Landau-level separation at the Fermi level redistributes the electron states.

In the region $\Delta_B\sim k_BT$, the electron distribution in the k_x,k_y plane is no longer continuous near the Fermi energy due to the 2D nature of the GIC's. Therefore the integration in Eq. (24) for the orbital susceptibility has to include the effect of the redistribution of electrons. A zeroth-order approximation for this correction to $\chi_{\rm orb}$ can be calculated by the following method. We replace the integration limits 0 to 3 in Eq. (24) by the interval ϵ_F^n to ϵ_F^{n+1}, where $\epsilon_F^n\equiv E_F^n/\gamma_0=\sqrt{2(n+1)B}/\gamma_0$, and $\epsilon_F^n\le E_F/\gamma_0<\epsilon_F^{n+1}$. The integration over the Landau levels adjacent to the Fermi energy gives the correction to the orbital susceptibility. Defining the correction term as $\delta\chi_{\rm orb}$, we obtain[12]

$$\delta\chi_{\rm orb}\simeq-\left[\frac{e}{\hbar c}\right]^2\frac{N_A\Omega\gamma_0a^2}{16\pi}(1+\gamma)\frac{\Delta_B}{k_BT} \quad (25)$$

for $k_BT>\Delta_B$, and

$$\delta\chi_{\rm orb}\simeq-\left[\frac{e}{\hbar c}\right]^2\frac{N_A\Omega\gamma_0a^2}{16\pi}(1+\gamma)\left[1-\frac{\Delta_B}{E_F}\right] \quad (26)$$

for $k_BT<\Delta_B$.

A semiemperical solution which satisfies both Eqs. (25) and (26) can therefore be written as

$$\delta\chi_{\rm orb}\simeq-\left[\frac{e}{\hbar c}\right]^2\frac{N_A\Omega\gamma_0a^2}{16\pi}(1+\gamma)\frac{\Delta_B}{k_B(T+T_s)}$$
$$=(-4.18\times10^{-6})(1+\gamma)\frac{\Delta_B}{k_B(T+T_s)}, \quad (27)$$

where $T_s\equiv\Delta_B/k_B$ and Eq. (27) is in units of emu/(mol of C). Note that in the high-temperature limit we recover Eq. (25), while in the low-temperature limit we obtain Eq. (26). Also note that $|\delta_{\rm orb}(T_s)|=\frac{1}{2}|\delta_{\rm orb}(0)|$ from Eq. (27), so that T_s can be estimated from experiments using the definition of Eq. (7). The theoretical fits using Eq. (27) for the experimental data are denoted by the solid lines in Figs. 1–4. The T_s values obtained from the fits are listed in Table II. For $T=T_s\equiv\Delta_B/k_B$, the Fermi energy yields the relation

$$E_F\simeq\frac{B}{k_BT_s}, \quad (28)$$

from Eq. (27). The Fermi energies thus estimated for various K-GIC's and KH_x-GIC's are listed in Table II. Note that these values are generally in good agreement with the optical measurements.[13]

The magnitude of the temperature-dependent variation of the magnetic susceptibility $(\delta\chi_{\rm orb})_{\rm tot}$ at low temperatures can be obtained from Eq. (27):

$$(\delta\chi_{\rm orb})_{\rm tot}\equiv\delta\chi_{\rm orb}(T=0)-\delta\chi_{\rm orb}(T\gg T_s)$$
$$=(-4.18\times10^{-6})(1+\gamma)\frac{\Delta_B}{k_BT_s}$$
$$\approx-4.8\times10^{-6}\ \text{emu/(mol of C)}. \quad (29)$$

The total change of the susceptibility $(\delta\chi_{\rm orb})_{\rm tot}$ for KH_x-GIC's is estimated from the fits of the experimental data (see Figs. 1 and 2), which yields $(\delta\chi_{\rm orb})^{\rm expt}\simeq-4.0\times10^{-6}$ emu/(mol of C) for stage 1 and $\simeq-4.6\times10^{-6}$ emu/(mol of C) for stage 2, in good agreement with the theoretical value $(\delta\chi_{\rm orb})_{\rm tot}\simeq-4.8\times10^{-6}$ emu/(mol of C) within experimental error. Note that the magnitude of $\delta\chi_{\rm orb}$ is larger for higher stages in units of emu/(g of sample), because of the larger concentration of carbon in higher-stage GIC's. However, it should be pointed out that the magnitude of the susceptibility of GIC's should be compared in units of emu/(mol of C) because the orbital susceptibility of the Bloch electrons is calculated for the π electrons of the graphite.

The temperature dependence of $\delta\chi_{\rm orb}(T)$ for a constant Fermi energy and at various constant magnetic fields is shown in Fig. 7, and that for various Fermi energies at a constant magnetic field is shown in Fig. 8. Note that $|\delta\chi_{\rm orb}|$ is only significant in the low-temperature and high-magnetic-field limit, and decreases rapidly with increasing T for large values of E_F.

As described previously, we may estimate the chemical potential of the interior graphite layers from the increase of the paramagnetism in the high-stage K-GIC's ($n\ge3$) in the low-temperature and low-magnetic-field limit. Assuming that the enhancement of the paramagnetism in the high-stage K-GIC's (see Fig. 6 for stage-3 and -4 K-GIC's) is completely due to the interband transitions of electrons in the interior graphite layers, the magnetic-

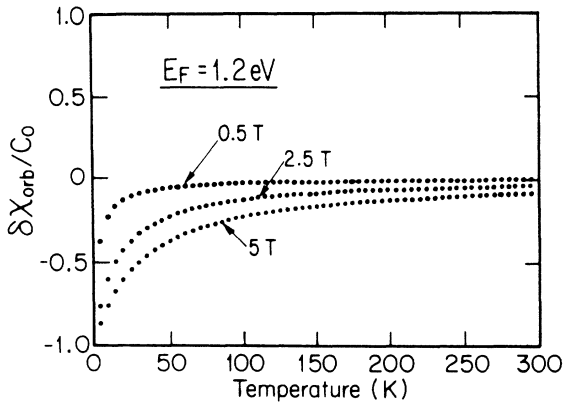

FIG. 7. The temperature variations in the magnetic susceptibility $[\delta\chi_{orb}(T)/C_0]$ with a constant Fermi energy ($E_F = 1.2$ eV) at magnetic fields $H = 0.5$, 2.5, and 5.0 T. Here, $C_0 \equiv (e/\hbar c)^2(3N_A\Omega\gamma_0 b^2/16\pi)$. Note that the magnitude of $\delta\chi_{orb}(T)$ is greater for larger H.

susceptibility contribution χ_{in} for interior layers is only measurable at high temperatures according to Eq. (5). Therefore the total difference in the magnetic susceptibility between that at low T and that at high T for the interior layers is approximately

$$\chi_{in}(T \ll T_0)|_{H\to 0} - \chi_{in}(T_0)|_{H\to 0} \equiv \delta\chi_{in} \simeq \frac{0.044}{k_B T\rho}\left[\frac{4}{\pi I_c}\right]^{3/2} \times (\gamma_0 a)^2\left[\frac{e}{\hbar c}\right]^2 \mathrm{sech}^2\left[\frac{\mu_{in}}{2k_B T_0}\right], \tag{30}$$

where ρ is the density, T_0 is an empirical characteristic temperature defined in Eq. (8), and I_c is the c-axis repeat distance of a GIC. From the values of $\delta\chi_{in}$ obtained from the experimental data in Fig. 6 for stage-3 and -4 K-GIC's, the effective chemical potentials (μ_{in}) of the interior graphite layers[6] for the high-stage K-GIC's can be estimated using Eq. (30). We obtain $\mu_{in} \approx 0.14$ eV for stage-3 K-GIC's and 0.09 eV for stage-4 K-GIC's. The screening length (λ^{-1}) can also be estimated from the known bounding-layer Fermi energy (E_F) according to the following form:

$$\frac{\mu_{in}}{E_F} = e^{-\lambda c_0}, \tag{31}$$

where c_0 is the interlayer seperation. The reciprocal screening length thus obtained is $\sim 7\times 10^7$ cm^{-1} for both $C_{36}K$ and $C_{48}K$.

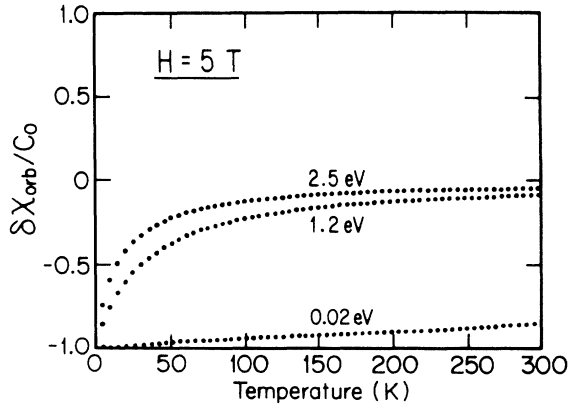

FIG. 8. The temperature variations in the magnetic susceptibility $[\delta\chi_{orb}(T)/C_0]$ at a constant magnetic field ($H = 5$ T) and with Fermi energies $E_F = 2.5$, 1.2, and 0.02 eV. Here, $C_0 \equiv (e/\hbar c)^2(3N_A\Omega\gamma_0 b^2/16\pi)$. Note that the magnitude of $\delta\chi_{orb}(T)$ is greater for smaller E_F.

VI. DISCUSSION

In the preceding section we presented a semiempirical calculation to explain the temperature dependence of $\chi_\parallel$ in donor-GIC's. The basic concept of the calculation lies in considering the discontinuous electron distributions in a magnetic field. The discontinuous energy spectrum has effects on the orbital magnetic susceptibility in the high-magnetic-field and low-temperature limit. This consideration was not previously discussed because various experimental and theoretical studies on the magnetic susceptibility of K-GIC's (Refs. 5, 6, and 8) were performed in the low-magnetic-field limit.

It is important to point out that our calculations for $(\delta\chi_\parallel)_{orb}$ are valid only for the bounding graphite layers and do not take account of the interlayer parameters. In contrast, the calculation for $\delta\chi_{in}$ is valid for the interior graphite layers which are screened by the charge in the bounding layers. Consequently, the $\delta\chi_{orb}(T)$ calculations are appropriate for stage-1 donor-GIC's, while that for $\delta\chi_{in}$ is a fairly good approximation for higher-stage donor-GIC's with stage index $n \geq 3$. For the intermediate condition, where $n = 2$, there are two graphite bounding layers between each two consecutive intercalate layers. In contrast to the case in stage-1 GIC's, there are direct interactions between these two bounding layers in stage-2 GIC's. Therefore the interlayer graphene tight-binding parameters γ_3 and γ_4, which describe the coupling between nearest interlayer carbon sites and are of the order of 0.1 eV in graphite, should be important for explaining the T and H dependence of the c-axis magnetic susceptibility in stage-2 GIC's. The high-field data $\chi_\parallel(T)$ for stage-2 GIC's behave similarly to those of stage-1 GIC's (Figs. 1–4), but show an enhanced paramagnetism at low T and small H that cannot be explained directly by either the calculation for $\delta\chi_{orb}(T)$ or that for $\delta\chi_{in}$. Calculations which include γ_3- and γ_4-type interactions may provide a possible explanation for the anomalous temperature dependence in stage-2 donor-GIC's. But the explicit calculations are complicated, and were not carried out in this work. Another possibility for explaining the temperature dependence of the susceptibility for the stage-2 K-GIC and stage-2 KH_x-GIC at low magnetic field may be the inhomogeneity in the samples.

The above interpretation of the experimental data is applicable to the bulk electronic properties. However, in

the case of KH_x-GIC's, there are other physical properties associated with the hydrogen ratio x that should be considered. For large x ($x \geq 0.1$) in the chemisorbed KH_x-GIC's, charge transfer from potassium to hydrogen is nearly complete, and therefore hydrogen is expected to be in the H^- form.[9,24] In contrast, for a small hydrogen concentration ($x < 0.1$), the hydrogen species in the KH_x-GIC's are physisorbed and are mostly in the molecular form H_2^- at low temperatures (e.g., less than liquid-N_2 temperatures).[24] Consequently, there is a free spin for each H_2^- molecular unit, which should provide a Curie-type paramagnetic contribution. Thus, the magnetic-susceptibility data should exhibit a Curie-type temperature dependence for physisorbed KH_x-GIC's as well as chemisorbed KH_x-GIC's with incomplete charge transfer. This interpretation may explain the temperature dependence of the magnetic susceptibility obtained from electron-spin-resonance (ESR) measurements,[24] which are sensitive to the presence of localized spins. Although the ESR measurements provide useful information on the charge surrounding the hydrogen species, these measurements are not sensitive to the bulk susceptibility of the system. Also note that the Curie-type paramagnetism in the chemisorbed KH_x-GIC's due to incomplete charge transfer is much smaller than the bulk susceptibility [typically of the order of 10^{-9} emu/(g of sample)], and therefore can be neglected in the discussion of bulk properties.

Finally, we comment on the magnetic field dependence of the room-temperature susceptibility. According to Ref. 5, the room-temperature susceptibility in K-GIC's does not show a magnetic field dependence for $0.5 < H < 1.3$ T. Except for the measurement at 0.5 T, where our results agree with those of Ref. 5, the measurements reported in this work are taken in magnetic fields well above 1.3 T, where there is a field dependence.

VII. SUMMARY

Static magnetic-susceptibility measurements on nonmagnetic donor-type KH_x-GIC's and K-GIC's have been carried out. The anomalous temperature dependence in the limit $\Delta_B \sim k_B T$, where Δ_B denotes the Landau-level separation at the Fermi level, is shown to be the result of the inter-Landau-level transitions in these quasi-two-dimensional metallic systems. By calculating an expression for the temperature dependence of the susceptibility, we show that the low-temperature–high-field anomaly provides a possibility for probing the Fermi energies of these layered compounds.

The absolute values of the room-temperature magnetic susceptibility in these donor-GIC's are also studied. The enhanced Pauli spin susceptibility based on Fermi-liquid theory is formulated using available experimental parameters, and the enhancement in shown to be important in accounting for the discrepancy between the calculated orbital susceptibility and the experimental data. The magnetic susceptibility of KH_x-GIC's exhibit interesting contrasts to that of K-GIC's, because the charge transfer to hydrogen greatly reduces the carrier density in the graphite π conduction bands as well as the c-axis charge inhomogeneity in the case of the KH_x-GIC's.

The increase in the paramagnetism at low temperature in higher-stage donor-GIC's ($n \geq 3$) is shown to be related to the screened chemical potential of the interior graphite layers. We therefore estimate the chemical potentials of the interior graphite layers in the case of stage-3 and stage-4 K-GIC's, as well as the screening lengths in these compounds.

The above discussion can be generalized and applied to other layered quasi-two-dimensional metallic systems, provided that the band structures are known.

ACKNOWLEDGMENTS

This work was submitted by N.-C. Y. in partial fulfillment of the requirements of the Ph.D. degree at the Massachusetts Institute of Technology (1988). The authors are grateful to Dr. T. Enoki at the Tokyo Institute of Technology in Japan for his valuable discussion and his help with the sample preparation. The magnetic-susceptibility measurements were performed using the SQUID at the Francis Bitter National Magnet Laboratory (FBNML) at MIT. We also thank Dr. R. Frankel at the FBNML for his technical assistance and discussions. This work was supported by U.S. Air Force Office of Scientific Research Contract No. F49620-83-C-0011 during its early phases and by U.S. National Science Foundation Grant No. 83-10482DMR in the later phases.

*Also with the Department of Physics, Massachusetts Institute of Technology, Cambridge, MA. Present address: IBM Research Division, Thomas J. Watson Research Center, P.O. Box 218, Yorktown Heights, NY 10598.

†Present address: College of Pharmacy, Nihon University, 7-chome 7-1 Narashino-dai, Funabashi, Chiba 274, Japan.

‡Also with the Departments of Physics and Electrical Engineering and Computer Science, Massachusetts Institute of Technology, Cambridge, MA.

[1]L. D. Landau, Z. Phys. **64**, 629 (1930) [English translation in *Collected papers of L. D. Landau*, edited by D. ter Haar (Gordon and Breach, New York, 1965).

[2]R. Peierls, Z. Phys. **80**, 763 (1933).

[3]H. Fukuyama, Prog. Theor. Phys. **45**, 704 (1971).

[4]J. W. McClure, Phys. Rev. **104**, 666 (1956).

[5]F. J. DiSalvo, S. A. Safran, R. C. Haddon, J. V. Waszczak, and J. E. Fisher, Phys. Rev. B **20**, 4883 (1979).

[6]S. A. Safran and F. J. DiSalvo, Phys. Rev. B **20**, 4889 (1979).

[7]J. Blinowski and C. Rigaux, J. Phys. (Paris) **45**, 545 (1984).

[8]R. Saito, Ph.D. thesis, University of Tokyo, 1984.

[9]T. Enoki, N. C. Yeh, S. T. Chen, and M. S. Dresselhaus, Phys. Rev. B **33**, 1292 (1986).

[10]T. Enoki, N. C. Yeh, G. Roth, G. Dresselhaus, and M. S. Dresselhaus, in *Extended Abstracts of the 17th Biennial Conference on Carbon*, edited by P. C. Eklund (American Carbon Society, State College, PA, 1985), p. 196.

[11]N. C. Yeh, T. Enoki, L. Salamanca-Riba, and G. Dresselhaus, in *Layered Structures and Epitaxy, MRS Symposia Proceedings, Boston*, edited by J. M. Gibson, G. C. Osbourn, and R. M. Tromp (Materials Research Society, Pittsburgh, 1986),

Vol. 56, p. 467.
[12]N. C. Yeh, Ph.D. thesis, Massachusetts Institute of Technology, 1988.
[13]G. L. Doll, M. H. Yang, and P. C. Eklund, Phys. Rev. B **35**, 9790 (1987).
[14]M. Zanini and J. E. Fischer, Mater. Sci. Eng. **31**, 169 (1977).
[15]L. D. Landau, Zh. Eksp. Teor. Fiz. **32**, 59 (1957) [Sov. Phys.—JETP **5**, 101 (1957)].
[16]V. P. Silin, Zh. Eksp. Teor. Fiz. **33**, 1227 (1957) [Sov. Phys.—JETP **6**, 945 (1958)].
[17]R. M. White, in *Quantum Theory of Magnetism,* Vol. 32 of *Springer Series in Solid-State Sciences,* edited by M. Cardona, P. Fulde, and H. Queisser (Springer, New York, 1983).
[18]J. Hubbard, Proc. R. Soc. London, Ser. A **276**, 238 (1963).
[19]K. Higuchi, H. Suematsu, and S. Tanuma, J. Phys. Soc. Jpn. **48**, 1532 (1980).
[20]G. Dresselhaus, S. Y. Leung, M. Shayegan, and T. C. Chieu, Synth. Met. **2**, 321 (1980).
[21]S. Tanuma, H. Suematsu, K. Higuchi, R. Inada, and Y. Onuki, in *Applications of High Magnetic Fields in Semiconductor Physics,* edited by J. F. Ryan (Clarendon, Oxford, 1978), p. 85.
[22]J. C. Slonczewski and P. R. Weiss, Phys. Rev. **109**, 272 (1957).
[23]J. W. McClure, Phys. Rev. **108**, 612 (1957).
[24]T. Enoki, S. Miyajima, M. Kabasawa, T. Chiba, H. Yamamoto, H. Inokuchi, and K. Seki, *MRS Extended Abstracts,* edited by M. Endo, M. S. Dresselhaus, and G. Dresselhaus (MRS Society, Pittsburgh, PA, 1988), p. 213.